

Static and dynamic responses of Halgavor Footbridge using steel and FRP materials

M. Gunaydin ^{*1}, S. Adanur ², A.C. Altunisik ^{2a} and B. Sevim ³

¹ Department of Civil Engineering, Gümüşhane University, Gümüşhane, Turkey

² Department of Civil Engineering, Karadeniz Technical University, Trabzon, Turkey

³ Department of Civil Engineering, Yıldız Technical University, İstanbul, Turkey

(Received July 18, 2013, Revised April 30, 2014, Accepted May 12, 2014)

Abstract. In recent years, the use of fiber reinforced polymer composites has increased because of their unique features. They have been used widely in the aircraft and space industries, medical and sporting goods and automotive industries. Thanks to their beneficial and various advantages over traditional materials such as high strength, high rigidity, low weight, corrosion resistance, low maintenance cost, aesthetic appearance and easy demountable or moveable construction. In this paper, it is aimed to determine and compare the geometrically nonlinear static and dynamic analysis results of footbridges using steel and glass fiber reinforced polymer composite (GFRP) materials. For this purpose, Halgavor suspension footbridge is selected as numerical examples. The analyses are performed using three identical footbridges, first constructed from steel, second built only with GFRP material and third made of steel- GFRP material, under static and dynamic loadings using finite element method. In the finite element modeling and analyses, SAP2000 program is used. Geometric nonlinearities are taken into consideration in the analysis using P-Delta criterion. The numerical results have indicated that the responses of the three bridges are different and that the response values obtained for the GFRP composite bridge are quite less compared to the steel bridge. It is understood that GFRP material is more useful than the steel for the footbridges.

Keywords: finite element model; geometrically nonlinear static and dynamic analysis; glass fiber reinforced polymer; static analysis; suspension footbridge

1. Introduction

Traditional materials (concrete and steel) remained insufficient as a result of increasing demands of engineering applications. For this purpose, the composite materials were developed as of World War II and this development has continued rapidly since then. Nowadays, composite materials are commonly preferred in many engineering structures thanks to their beneficial properties and various advantages when these materials are compared to traditional ones. Fiber reinforced polymer (FRP) is a class of advanced composite materials used in civil engineering since the construction of the first all composite bridge Miyun, China, in 1982.

The use of FRP composite materials are gaining popularity for bridge application worldwide

*Corresponding author, Ph.D., E-mail: gunaydin61@hotmail.com.tr

and they have been used to build deck, beams, cables and superstructures of suspension bridge, footbridge and highway bridges. There are 355 bridges where the entire bridge or some of the components like beams, cables, tendons, deck and piers are constructed from FRP materials by the year 2003 and a number of bridges built after 2003 (Potyrala 2011). The first FRP composite bridge in the world was constructed in Ginizi, Bulgaria in 1981 using hand lay-up technique (Adanur *et al.* 2011). The second road bridge was the Miyun Highway Bridge with a span of 20.7m and a width of 9.2m. This bridge was built in China on October 1982 using a box-beam made of GFRP honeycomb plates (Shrivastava *et al.* 2009).

The idea of the use of composites for constructing long-span suspension and cable-stayed bridges was offered in mid 1980s by the Swiss Federal Laboratories for Materials Testing and Research (Meier 1987). The Stork Bridge is one of the first applications of the CFRP cables which were built in Switzerland in 1996 (Adanur *et al.* 2011). The Aberteldy Bridge built in Scotland and crosses over River Tay. The bridge is considered to be the first all-composite cable-stayed footbridge and the longest span all-composite footbridge in the world.

Footbridges manufactured from FRP composites are considered as alternatives to steel and concrete. Thus, understanding of the static and dynamic behavior of the FRP footbridges is becoming more important. Khalifa *et al.* (1996) described the analysis and design methodology for an FRP cable-stayed pedestrian bridge. In the study, the behaviors of the bridge under the static and dynamic loads were investigated. Hodhod and Khalifa (1997) investigated the dynamic characteristics and the seismic response of an FRP cable-stayed footbridge and compared its results to a conventional steel-concrete cable-stayed footbridge. Szak *et al.* (1999) studied the Clear Creek hybrid composite I-Girder pedestrian bridge. The design and performance of a modular fiber reinforced plastic bridge were studied by Aref and Parsons (2000). Burgueno *et al.* (2001) examined the experimental dynamic characterization of an FRP composite bridge superstructure assembly. Meiarashi *et al.* (2002) exhibited the results of a life-cycle cost analysis for two suspension bridges with same dimensions that were made of conventional steel and advanced all-composite CFRP composites. It was concluded that the composite bridge becomes more lifecycle cost-effective compared to the conventional steel bridge. The dynamic responses of three fiber reinforced polymer composite bridges were presented by Aluri *et al.* (2005). Caron *et al.* (2009) described the self stressed bowstring footbridge in FRP. In the study, static and dynamic behavior of the bridge was discussed. Chen *et al.* (2009) investigated the experimental characterization and optimization of hybrid FRP/RC bridge superstructure system. The experimental investigation was done to test the performance of a bridge system. Adanur *et al.* (2010) presented the comparison of analysis results of footbridges using steel and CFRP materials. In the study, displacement and internal forces obtained from the bridge deck and column were compared with each other. It was concluded that CFRP is more effective than steel. Jin *et al.* (2010) studied the dynamic characteristics of light-weight FRP footbridge. In the study, a tentative FRP cable-stayed bridge was investigated. Also, the design method and indices for FRP footbridges were also studied. Wang and Wu (2010) studied the integrated high-performance thousand-metre scale cable-stayed bridge with hybrid FRP cables. In this resent study, the suitability of hybrid basalt and carbon FRP cables instead of steel cables was investigated. It is aimed to eliminate the limitations of conventional steel stay cables in a long span cable-stayed bridge. Elsafi *et al.* (2012) presented dynamic analysis of the Bentley Creek Bridge with FRP deck. The bridge is located in Wellsburg, Chemung County, New York. It has truss steel structure with concrete deck of 42.7 m long. The concrete deck was replaced in 1999 with FRP deck. The dynamic behavior of concrete and FRP bridge deck were determined and results were compared with each other. Wang *et al.*

(2013) studied about the use of new composite material, basalt FRP which offers potential advantages for application in long-span cable-stayed bridges.

The objective of this paper is to evaluate both the geometrically nonlinear static and dynamic responses of an FRP composite suspension footbridge and compare these responses to an identical steel bridge. To this end, a suspension footbridge is selected and, static and dynamic finite element analyses are carried out. Similar analytical procedures are also performed on an identical bridge made of FRP composite elements in lieu of steel elements, with the same cross-sectional areas.

2. Numerical application

2.1 Description of the suspension footbridge

The Halgavor suspension footbridge (Fig. 1) is located over the busy A 30 dual carriageway in the south of Bodmin in Cornwall, UK. This bridge was constructed in 2001 having a total span of 47 m. The Halgavor Bridge is the first publicly funded bridge in the UK to use glass fibre reinforced polymer composites (GFRP) as the principal structural material. A glass-reinforced vinyl ester resin composite deck is suspended from a conventional primary support system comprising steel masts, steel spiral strand main cables and stainless steel hangers (Firth and Cooper 2002).

The bridge deck was built in the form of sandwich construction with 10×10 m panels. Each panel has a wide and thickness of 3.5 m and 37 mm, respectively. The completed bridge surface was chosen with a rubber layer made from recycled car tires. This choosing enables it to be used by the pedestrians, horses and cyclists easily. In addition, rubber surface is not affected even under corrosive influence of horse urine like a steel and concrete. The Halgavor bridge deck is given in Fig. 2.

2.2 Analytical model of the Halgavor Suspension Footbridge

In order to investigate both the geometrically nonlinear static and dynamic responses of the Halgavor suspension footbridge model, two-dimensional (2D) finite element model (Fig. 3) is modeled using SAP2000 software (SAP2000 2008). This program can be used for linear and



Fig. 1 Halgavor suspension footbridge (URL 2012a)



Fig. 2 Bridge deck of Halgavor suspension footbridge (URL 2012a)

non-linear, static and dynamic analyses of a 2D and 3D model of the structures. As the deck, pylons, and cables of the bridge are modeled by beam element, the hangers are modeled by truss elements. A finite element model (FEM) of the bridge with 92 nodal points, 102 beam elements and 10 truss elements are used in the analyses. The finite element model of the bridge is represented by 262 degrees of freedom. The material and section properties of the elements used in the finite element model are given in Table 1.

In this paper, three different finite element analyses are carried out to compare the geometrically nonlinear static and dynamic response of Halgavor Suspension Footbridge. For this purpose, steel and GFRP materials are used in the first and second analyses cases, respectively. In addition, the third analysis case performed on the existing bridge model having steel pylons, steel cables and

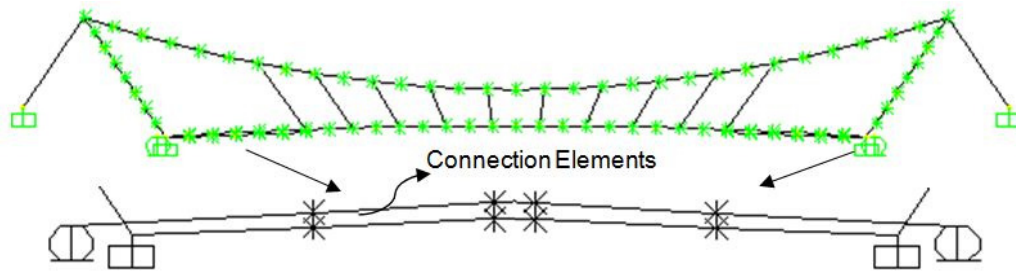


Fig. 3 Two-dimensional finite element model of Halgavor suspension footbridge

Table 1 Material and section properties of the element of Halgavor Suspension Footbridge

Member	Material properties				
	E (kN/m ²)	ν	A (m ²)	I (m ⁴)	ρ (kg/m ³)
Pylons	2.0500E8	0.30	0.14000	0.00292	7850
Deck	1.9875E7	0.30	0.26600	0.00418	3351
Cables	2.0500E8	0.30	0.02260	0.00002	7850
Hangers	2.0500E8	0.30	0.00565	0.00000	7850

* E : Modulus of elasticity; ν : Poisson's ratio; A : Section areas; I : Inertia moment; ρ : Density

Table 2 Material properties used analytical analyses of the footbridge

Structural elements		Material properties			
		Material	Modulus of elasticity (kN/m ²)	Directional symmetry type	Density (kg/m ³)
Case 1	Pylons	Steel	2.0500E8	Isotropic	7850
	Deck	Steel	2.0500E8	Isotropic	7850
	Cables	Steel	2.0500E8	Isotropic	7850
	Hangers	Steel	2.0500E8	Isotropic	7850
Case 2	Pylons	GFRP	0.8000E8	Orthotropic	2600
	Deck	GFRP	0.2100E8	Orthotropic	1900
	Cables	GFRP	0.8000E8	Orthotropic	2600
	Hangers	GFRP	0.8000E8	Orthotropic	2600
Case 3	Pylons	Steel	2.0500E8	Isotropic	7850
	Deck	GFRP	1.9875E7	Orthotropic	3351
	Cables	Steel	2.0500E8	Isotropic	7850
	Hangers	Steel	2.0500E8	Isotropic	7850

steel hangers and GFRP deck materials. Only materials properties are changed in the analyses with the same cross sectional areas. The values of the materials properties used in the analysis of the footbridge are given in Table 2. The material properties of the Case 2 were obtained from the literature (Votsis *et al.* 2005, Wang and Wu 2010).

3. Geometrically nonlinear behavior

Geometric nonlinearity of the structural elements should be taken into account in the analysis of bridges. Thus, geometric nonlinearity is considered for all analysis cases. The geometric nonlinearity occurred from self-weight of the bridges. This is achieved by performing finite element analysis considering the *P*-delta criteria.

Generally axial forces acting on the structures have little effect on the stiffness of structure when they are below certain values. But depending on the Young's modulus of the material, supporting conditions and inertial forces of the structural elements, axial forces can greatly contribute to stiffness and may cause nonlinear behavior of the structure. Consequently, total stiffness matrix of the system is the sum of elastic stiffness matrix and geometric stiffness matrix (Przemieniecki 1968).

$$K = K_E + K_G \quad (1)$$

where K_E and K_G are elastic and geometric stiffness matrices, respectively.

4. Modal analysis

Damping coefficients of the FRP composite structures are higher than those of typical steel

structures (Alampalli 2006). In the dynamic analysis, a damping ratio of %2 is considered for the steel bridge model, while a %5 damping ratio is used for the FRP composite bridge model. The modal analysis is solved to determine the frequency and mode shapes of the all bridge models. The first ten mode shapes and their frequencies were obtained from the modal analysis examined. Table 3 summarizes the frequencies and periods of the selected modes for all models. From Table 3, it can be seen that the frequencies exhibit some differences when compared with each other. Although GFRP composite bridge has lower self-weight than steel, relatively lower frequency

Table 3 First 10 modal frequencies and periods of the steel, GFRP and steel-GFRP bridges

Mod number	Steel bridge		GFRP bridge		Steel-GFRP bridge	
	F (Hz)	P (s)	F (Hz)	P (s)	F (Hz)	P (s)
1	2.449	0.408	2.022	0.494	1.770	0.565
2	2.590	0.387	2.164	0.462	1.927	0.520
3	4.031	0.248	4.040	0.248	3.448	0.289
4	5.335	0.187	4.364	0.229	3.891	0.257
5	6.084	0.164	6.390	0.156	4.976	0.200
6	8.798	0.114	6.660	0.150	6.186	0.161
7	10.576	0.095	9.845	0.101	7.493	0.133
8	10.637	0.094	11.570	0.086	10.346	0.096
9	13.467	0.074	11.663	0.085	10.697	0.093
10	17.600	0.056	14.018	0.071	11.154	0.089

* F : Frequency; P : Period

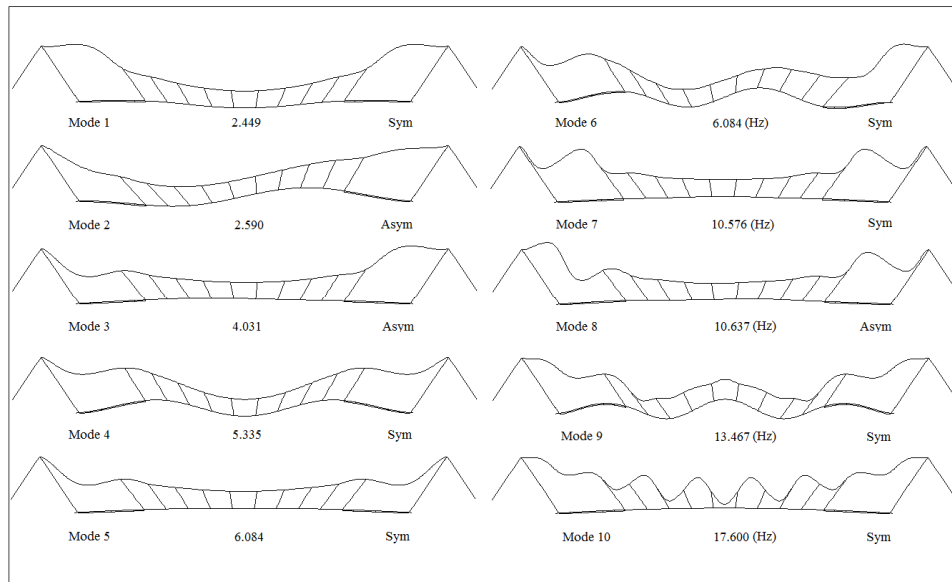


Fig. 4 First 10 mode shapes of the steel suspension footbridge

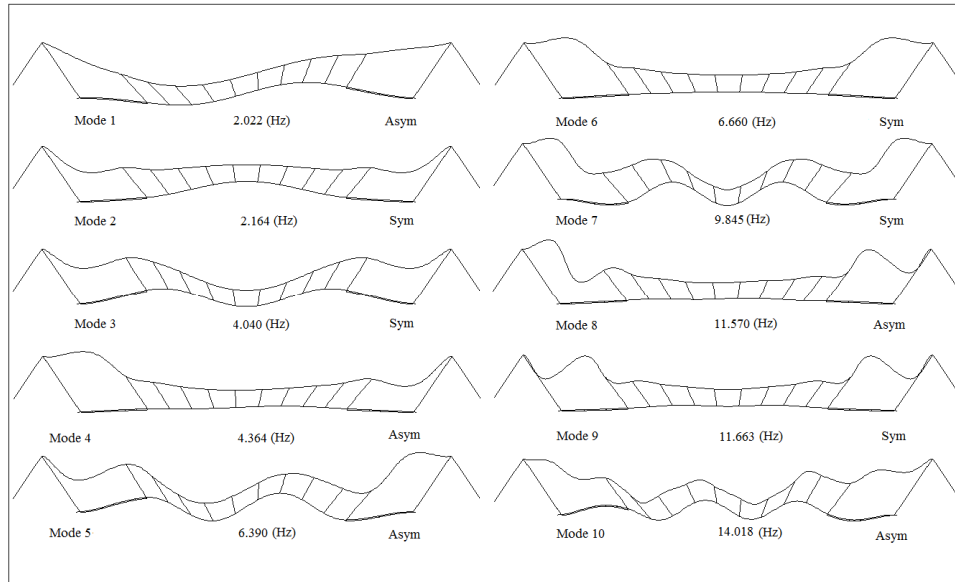


Fig. 5 First 10 mode shapes of the GFRP suspension footbridge

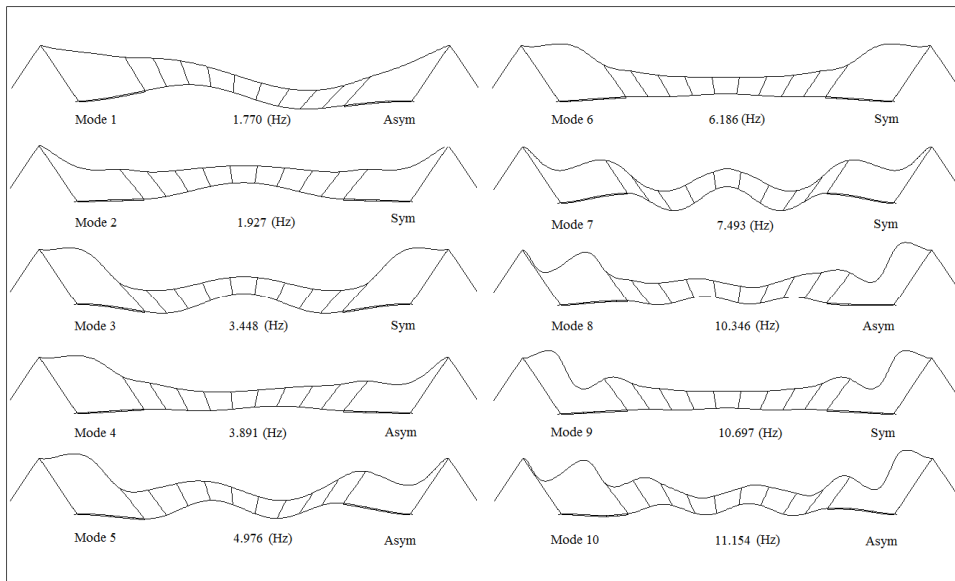


Fig. 6 First 10 mode shapes of the steel-GFRP suspension footbridge

values than steel have been obtained as a result of the modal analyses for the bridge which is contrary to expectations. It is thought that this situation has occurred as a consequence of bridge rigidity decrease depending upon the decreasing bridge mass. The first ten modes shape of the bridge models are also shown in Figs. 4-6. It is seen in these figures that three bridge models have generally similar mode shapes despite different mode sequences.

5. Geometrically nonlinear static analysis

Only self-weight of the footbridge is considered in the geometrically nonlinear static analysis as a load case to assess the differences. Because of the symmetrical nature of the bridge, the analysis was performed only one side of the bridge model. The variation of the displacement and internal forces obtained from the static analysis considering geometric nonlinearity for bridge pylon, deck and hangers are examined.

5.1 Pylon response

The distribution of the displacements and axial forces with the height of bridge pylon for Case 1, Case 2 and Case 3 are given in Fig. 7. Displacements increase with the height of the bridge pylon and displacements values obtained from all cases are nearly equal. The maximum displacement occurred as 0.85mm at the top of the bridge pylon.

Axial forces decrease along the height of the bridge pylon in all cases. The axial forces at the

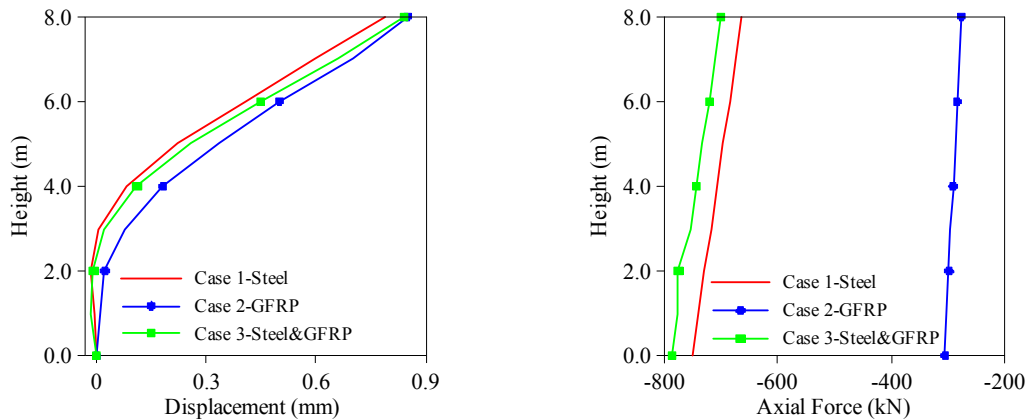


Fig. 7 Changing of displacements and axial forces along to bridge pylon

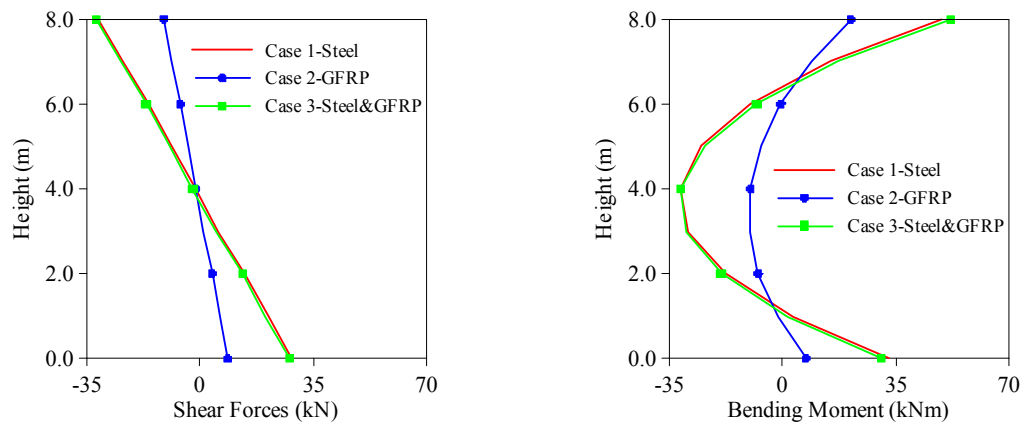


Fig. 8 Changing of shear forces and bending moments along to bridge pylon

base for Case 1, Case 2 and Case 3 bridge models are -752 kN, -305 kN and -700 kN, respectively. Numerical results indicates that the axial forces for the GFRP composite bridge model (Case 2) are less than those of the steel (Case 1) and steel-GFRP (Case 3) composite bridge model. Thus, GFRP material has an important effect on the axial forces.

Fig. 8 presents the shear forces and bending moments of the bridge pylon for Case 1, Case 2 and Case 3. It can be seen from the figure that the shear forces and bending moments corresponding to the GFRP composite bridge model are quite less compared to those of obtained from the steel (Case 1) and Steel-GFRP (Case 3) bridge model. It can easily be seen that the shear forces and bending moments values obtained Case 1 and Case 3 are nearly equal. Maximum shear forces and maximum bending moments occurred as -32 kN and 52 kNm for Case 1 and Case 3, respectively. But, the shear force and bending moment values for Case 2 were obtained 2.5 times less than the values of Case 1 and Case 3.

To determine the geometrically nonlinear analysis effect and to compare the results with static analysis, the finite element models of the bridge are reanalyzed. From the analyses, it is seen that the displacements obtained from the geometrically nonlinear analyses are bigger than those of the static analyses accounting for nearly the 14%, 18% and 8% for Case 1, Case 2 and Case 3, respectively. Axial forces obtained from the geometrically nonlinear analyses are bigger than those of the static analyses which are nearly the 17%, 13% and 7% for Case 1, Case 2 and Case 3, respectively. Shear forces obtained from both analyses are almost equal. Bending moments obtained from the geometrically nonlinear analyses are smaller than those of the static analyses nearly the 10%, 19% and 29% for Case 1, Case 2 and Case 3, respectively.

5.2 Deck response

The displacement obtained from the geometrically nonlinear static analysis at the deck for Case 1, Case 2 and Case 3 are given in Fig. 9. It is seen that displacements increase along the bridge deck and reach a maximum of 5.7 cm at the middle for the Case 3. Although the maximum displacement value occurred as 5.7 cm for Case 3, the displacement values obtained geometrically nonlinear static analysis is very close to each other for all cases.

Variation of shear forces and bending moments obtained from the geometrically nonlinear static analysis at the deck for all cases are given in Fig. 10.

As shown in this figure, the shear forces and bending moments values obtained from the geometrically nonlinear static analysis are nearly equal for Case 2 and Case 3. The maximum shear forces and bending moments occurred as 339 kN and 660 kNm for Case 1, respectively.

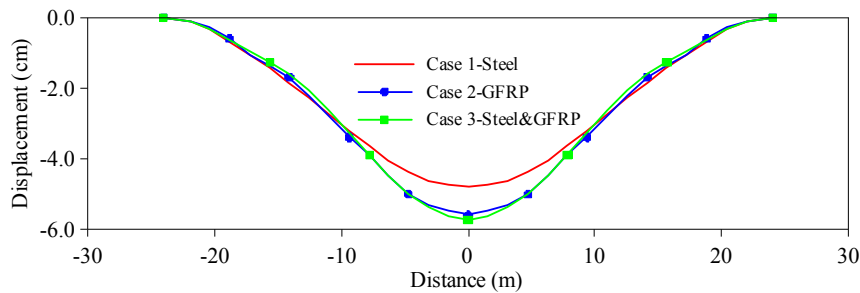


Fig. 9 Vertical displacements along the bridge deck

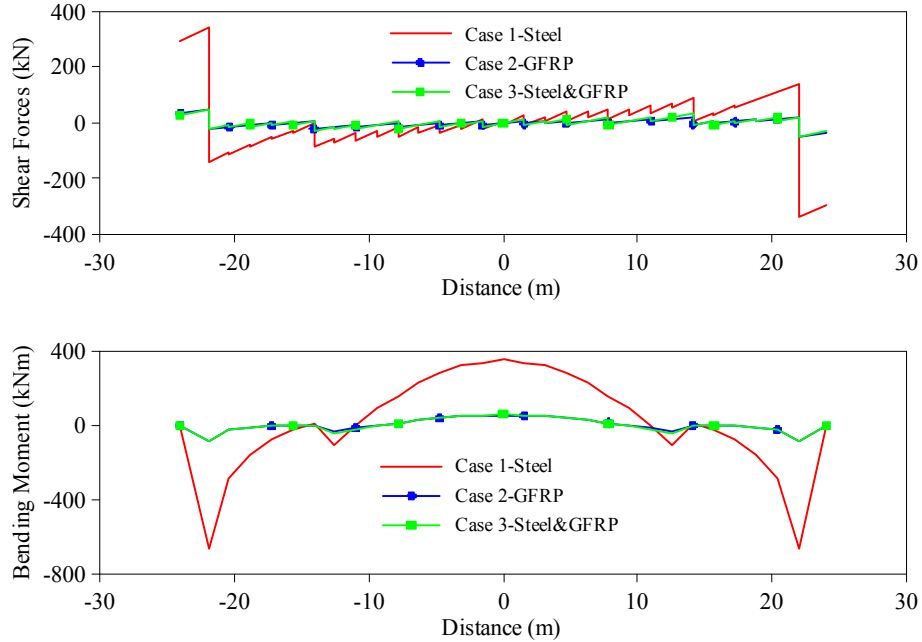


Fig. 10 Changing of the shear forces and bending moments along to bridge deck

Numerical results indicated that the GFRP material has an important effect on the shear forces and bending moments.

To determine the geometrically nonlinear analysis effect and to compare the results with static analysis, the finite element models of the bridge are reanalyzed. As shown in the analyses, the displacements in the geometrically nonlinear analyses are smaller than those in the static analyses which are approximately 3%, 12% and 20% for Case 1, Case 2 and Case 3, respectively. Similar to the displacement values above, shear forces obtained from the geometrically nonlinear analyses are smaller than those of the static analyses which are around 7%, 13% and 10% for Case 1, Case 2 and Case 3, respectively. Bending moments of the geometrically nonlinear analysis are also smaller than those of the static analyses being around 7%, 14% and 13% for Case 1, Case 2 and Case 3, respectively.

5.3 Hanger response

Comparison of hanger forces obtained from the geometrically nonlinear static analysis for Case 1, Case 2 and Case 3 is plotted in Fig. 11. As seen in this figure, the hanger forces values obtained for Case 1 and Case 3 are nearly equal for all hangers. The maximum forces on the hangers occurred as an almost 70 kN for Case 1 and Case 3. On the other hand, the maximum hanger forces obtained for Case 2 occurred as 30 kN. These values show that the hanger forces for the GFRP bridge model (Case 2) are less than those of the steel (Case 1) and Steel-GFRP (Case 3) bridge model. So, GFRP material is more effective than steel on the hanger forces of the footbridge as similar shear forces and bending moments.

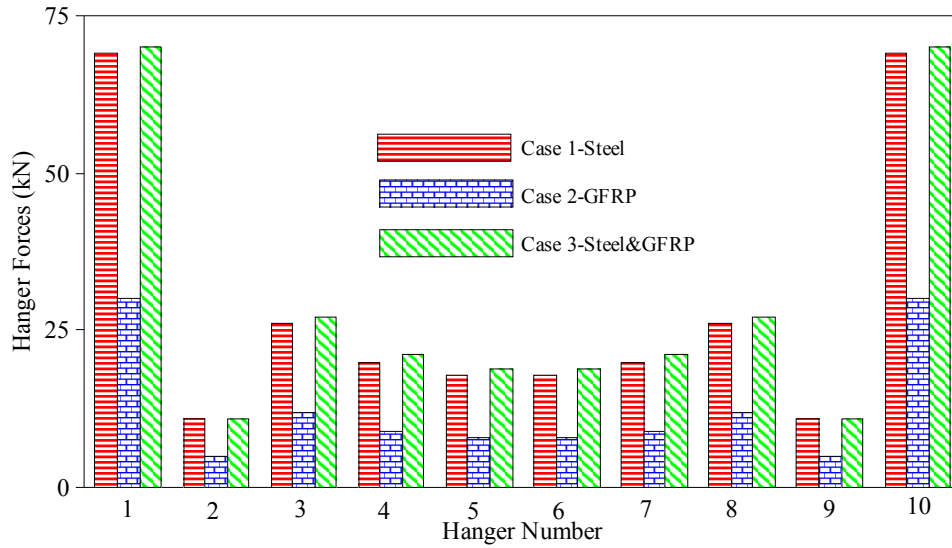


Fig. 11 Comparison of the hanger forces for all cases

To determine the geometrically nonlinear analysis effect and to compare the results with static analysis, the finite element models of the bridge are reanalyzed. From the analyses, it is seen that the hanger forces obtained from the geometrically nonlinear analysis are bigger than static analyses nearly the 17%, 7% and 2% for Case 1, Case 2 and Case 3, respectively.

6. Dynamic analysis

In the geometrically nonlinear dynamic analysis, the YPT330 component of Yarımcı station records of 1999 Kocaeli Earthquake (Fig. 12) (URL 2012b) is chosen as a ground motion. In this study, the only vertical component of the ground motion is applied to the bridge models in order to determine the dynamic behavior considering geometric nonlinearity of all bridge models. The absolute maximum response values of the steel, GFRP and steel-GFRP bridge models were examined for dynamic analysis to illustrate the differences between each model.

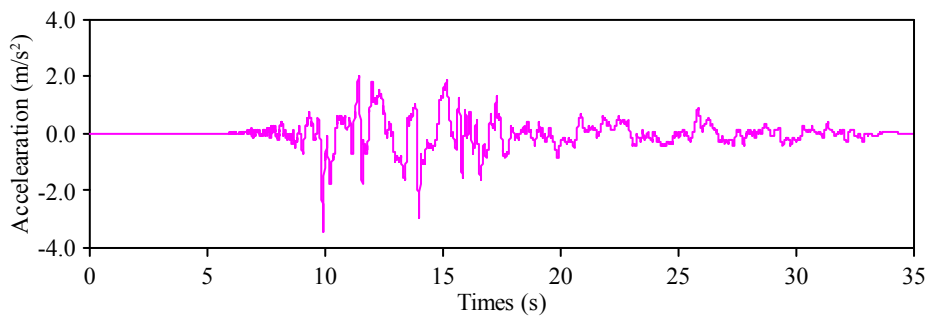


Fig. 12 The time-history of ground motion acceleration of 1999 Kocaeli earthquake

6.1 Pylon response

Fig. 13 shows the displacements and axial forces of the pylon obtained from the geometrically nonlinear dynamic analyses of the bridge models. As seen in these figures, the calculated displacement and axial forces for the Case 1 are bigger than the corresponding response obtained for the Case 2 and Case 3. At the top of the bridge pylon, GFRP composite bridge model underestimates the responses by 36% and 70% relative to the steel bridge model case for displacement and axial force respectively.

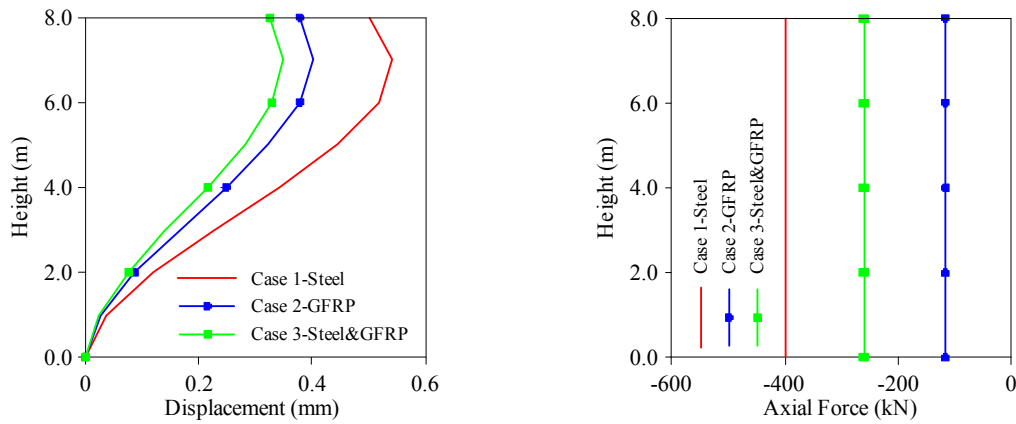


Fig. 13 Changing of dynamic displacements and axial forces along to bridge pylon

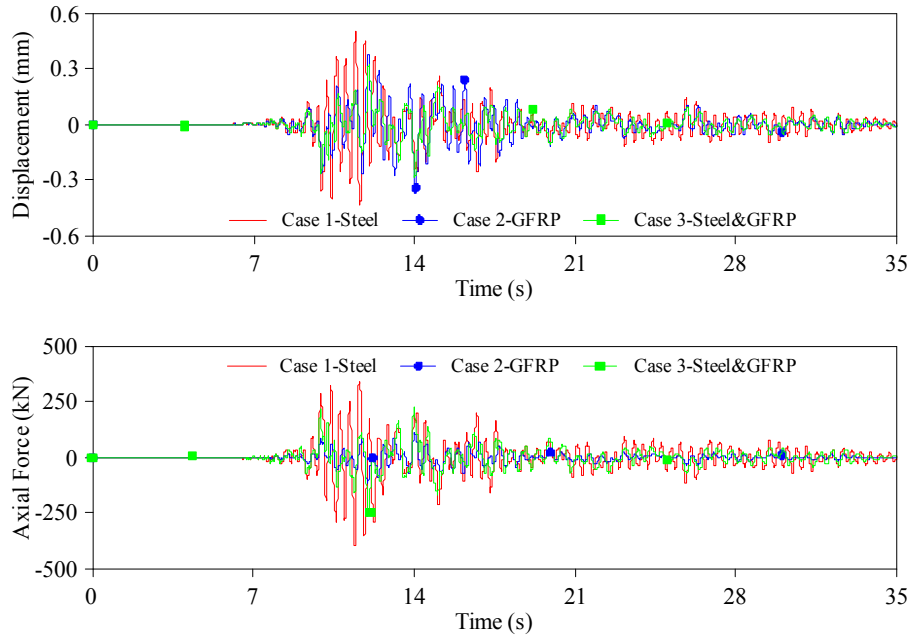


Fig. 14 The time histories of displacements and axial forces for all cases

The time histories of displacement and axial forces obtained from the geometrically nonlinear dynamic analysis at the top point of the bridge pylon and at the base of the pylon for all cases are shown in Fig. 14. From these figures, the maximum displacement at the top of the pylon is calculated as 0.5 mm at 11.43 s of the considered earthquake for Case 1, while the computed displacement for Case 2 and Case 3 are 0.37 mm at 11.98 s and 0.32 mm at 11.98 s.

The calculated axial forces at the base of -400 kN occurs at the 11.43 s for Case 1, while for the Case 2 and Case 3, the corresponding axial forces was -117kN and -266 kN which took place at 11.98 s and 12.01 s, respectively.

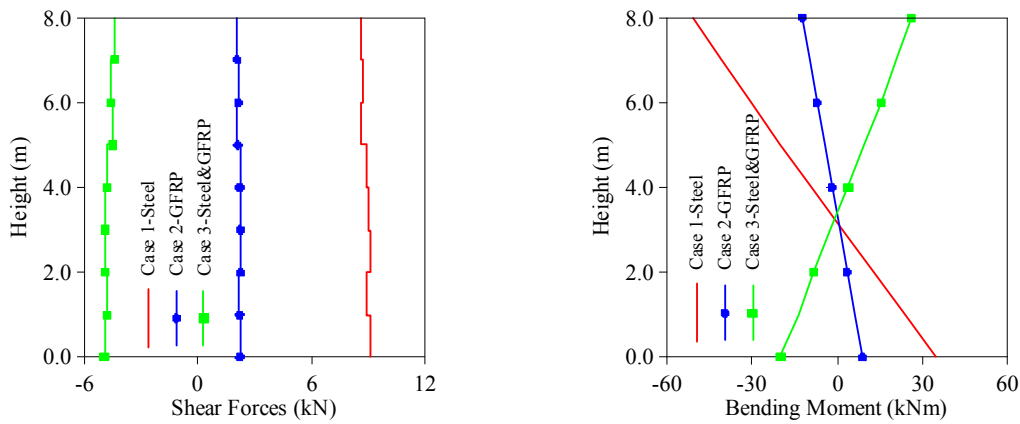


Fig. 15 Changing of shear forces and bending moments along to bridge pylon

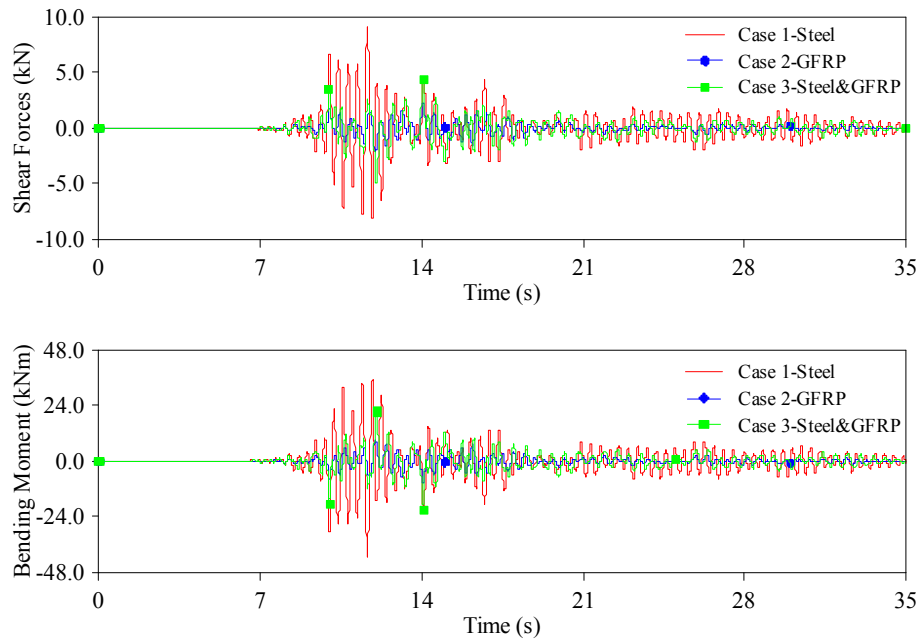


Fig. 16 The time histories of shear forces and bending moments for all cases

The shear forces and bending moments obtained from the geometrically nonlinear dynamic analysis of bridge models at the pylon are presented in Fig. 15. From these figures, it is clear that the shear forces and bending moments obtained for the steel bridge model are larger than the other ones. At the base of the bridge pylon, steel bridge model case overestimates the response by 76% relative to the GFRP bridge model case for shear force. In addition, steel bridge model overestimates the bending moment response by 75% relative to the GFRP bridge model at the top of the bridge pylon.

Shear force and bending moment time histories at the top of the bridge pylon for all cases are plotted in Fig. 16, respectively. It can be seen Fig. 16 that there is no close agreement between the time histories computed for the Case 1, Case 2 and Case 3 bridge models. This apparent discrepancy between the three bridge models time histories can be attributed to the variation of the materials properties in building each bridge models (Adanur *et al.* 2011).

6.2 Deck response

Fig. 17 points out the geometrically nonlinear dynamic displacements and its time histories at the middle point of the deck for the bridge models. It is seen from the Fig. 17 that the calculated displacement response values for the Case 1 is bigger than the corresponding response values obtained for the Case 2 and Case 3 as pylon response values. The maximum displacements occurred as -4.9 cm, -3.5 cm and -2.6 cm at the middle of the bridge deck for the Case 1, Case 2 and Case 3 respectively. In addition, the maximum displacement at the middle point of the deck is calculated as 4.9 cm at 11.64 s of the considered earthquake for Case 1, while the computed displacement for Case 2 and Case 3 are 3.5 cm at 14.08 s and 2.6 cm at 12.05 s, are shown in Fig.

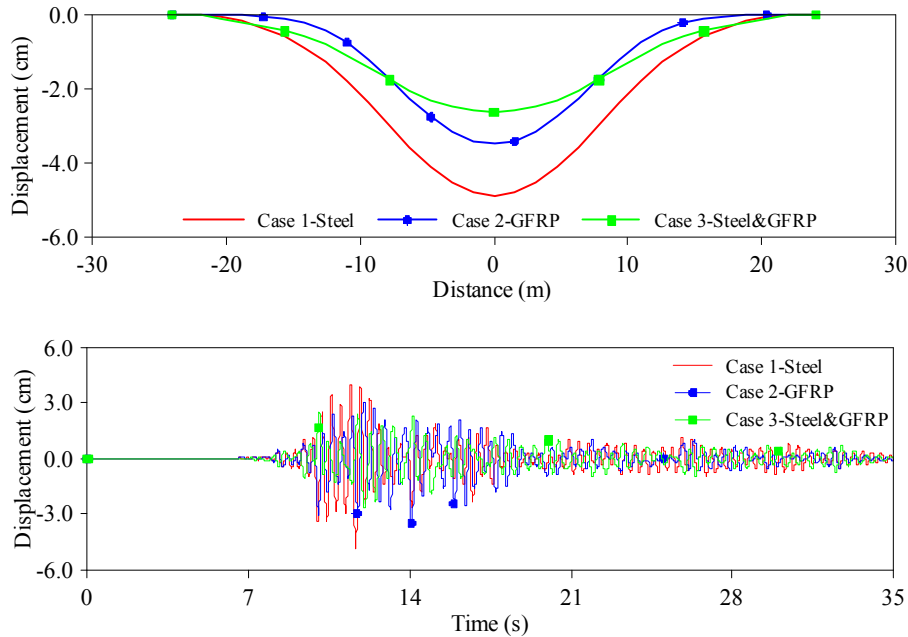


Fig. 17 The displacements and its time histories of the bridge deck for all cases

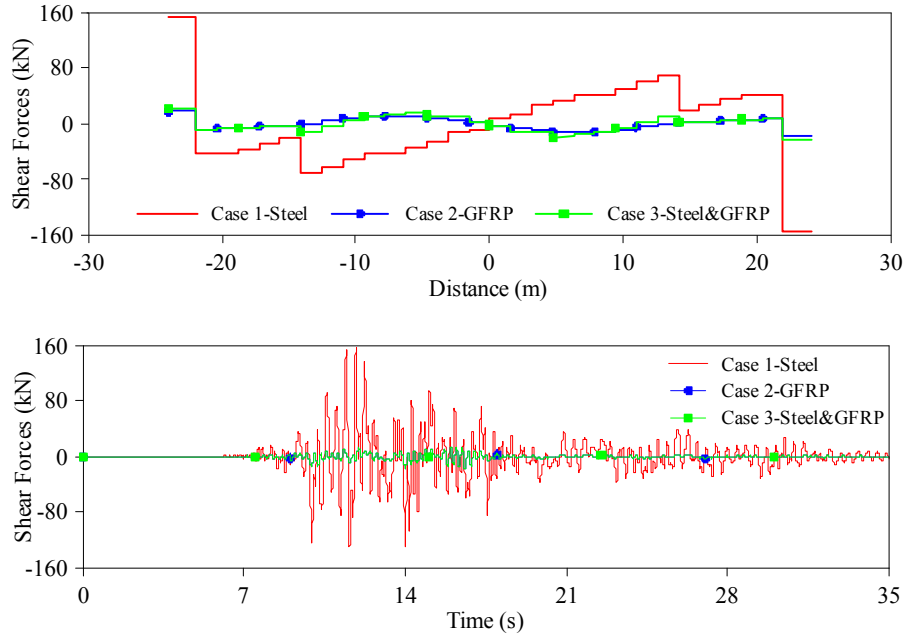


Fig. 18 The shear forces and its time histories of the bridge deck for all cases

17. The results indicate that the GFRP material is more effective than the steel on the displacements of the deck as similar pylon dynamic displacements.

Variation of shear forces obtained from the geometrically nonlinear dynamic analysis at the deck for all cases is plotted in Fig. 18. As shown in this figure, the shear forces response values obtained from Case 1 are quite larger than the corresponding response values obtained for the Case 2 and Case 3. The difference values of the maximum shear force between Case 1 and Case 2 are reached to approximately 88% at the abutment for the bridge deck. Besides, the maximum shear forces at the abutment of the bridge deck at the time of maximum response for all cases are given in Fig. 18. It is seen that the GFRP material is more effective than the steel on the shear forces of the deck as similar deck displacements.

Fig. 19 illustrates the values of bending moments along the bridge deck and its time histories for all cases. When Fig. 19 is examined, the bending moments obtained for the steel bridge model are quite larger than the values obtained for the GFRP bridge model. The differences are reached to approximately 90% at the middle of the bridge deck. The time histories of the bending moments subjected to YPT300 component of Yarımca station records for all cases is also presented in Fig. 19. Fig. 19 indicated that there is no close agreement between the time histories of bending moment computed for the Case 1, Case 2 and Case 3 bridge models as time histories of displacement, axial and time histories of shear forces.

6.3 Hanger response

Comparison of hanger forces obtained from the geometrically nonlinear dynamic analysis for bridge models is plotted in Fig. 20. As seen in this figure, GFRP material is more effective than the steel on the dynamic hanger forces as similar internal forces.

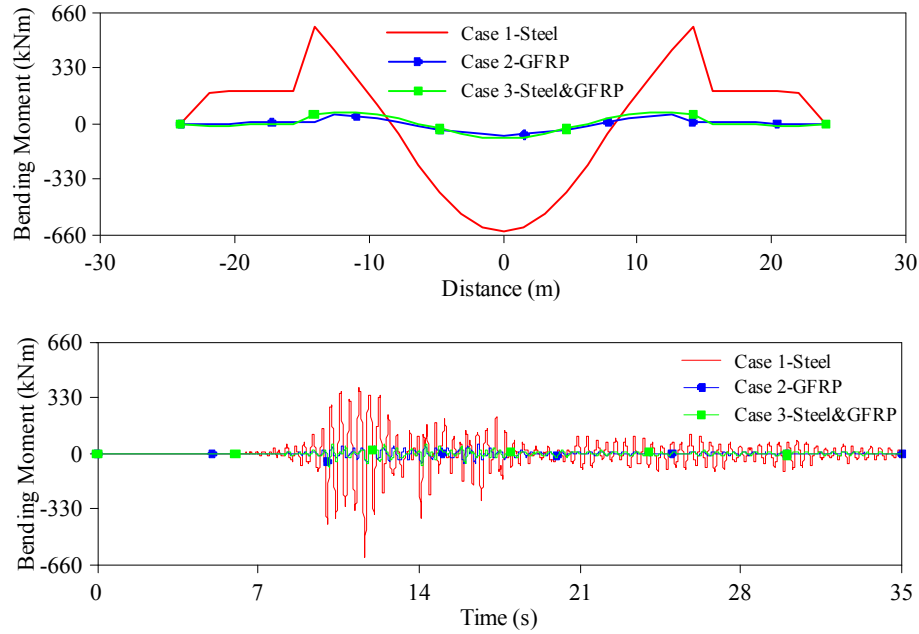


Fig. 19 The bending moments and its time histories of the bridge deck for all cases

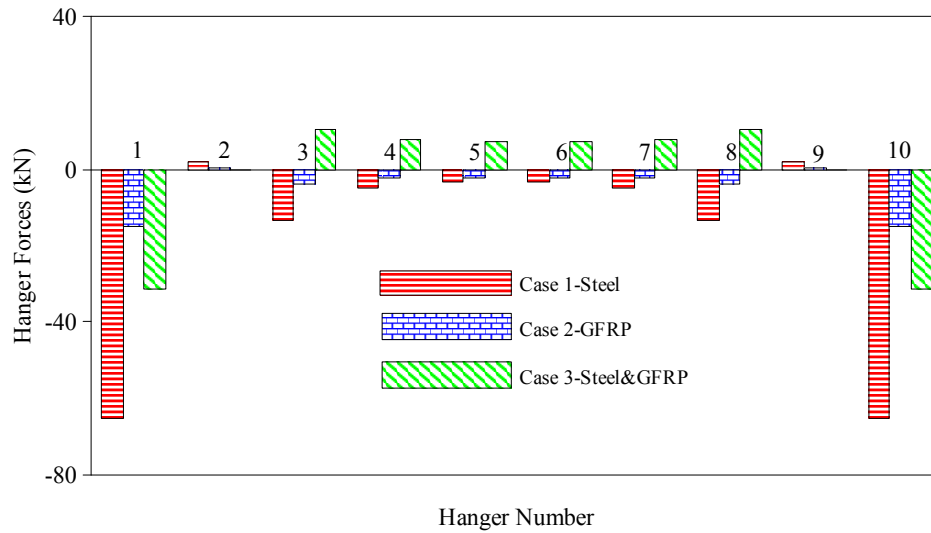


Fig. 20 Comparison of dynamic hanger forces for all cases

7. Conclusions

The aim of this article is to determine geometrically nonlinear static and dynamic responses of three models for a suspension footbridge which are made of steel, GFRP and steel-GFRP materials. Also, the static and dynamic analyses are performed to determine the geometrically nonlinear

analyses effects. For this purpose, Halgavor suspension footbridge is selected as case study. Two dimensional finite element model of the footbridge is created by SAP2000 software. Geometric nonlinearities are taken into consideration in the analysis using *P*-Delta criterion. Steel and GFRP materials are used in the first and second analyses cases, respectively. In addition, the third analysis case performed on the existing bridge model having steel pylons, steel cables and steel hangers and GFRP deck materials. Only materials properties are changed in the analyses, with the same cross sectional areas. YPT330 component of Kocaeli Earthquake is chosen in the dynamic analysis. Based on the results, the following observation can be made:

Modal analyses

- When the dynamic characteristics such as natural frequencies and mode shapes are compared with each other for all analyses, it can be seen that there is a same distribution between mode shapes. But the values of natural frequencies are different for all cases. The first ten modes are attained between 2.449 Hz - 17.600 Hz, 2.022 Hz - 14.018 Hz and 1.770 Hz - 11.154 Hz for Case 1, Case 2 and Case 3, respectively.

Geometrically nonlinear static analyses

- Displacements increase with the height of the bridge pylon and displacements values obtained from all cases are nearly equal. The maximum displacement occurred as 0.85 mm at the top of the bridge pylon.
- Axial forces decrease along the height of the bridge pylon in all cases. The axial forces at the base for Case 1, Case 2 and Case 3 bridge models are attained as -752 kN, -305 kN and -700 kN, respectively. Numerical results indicate that GFRP material has an important effect on the axial forces.
- The shear forces and bending moments corresponding to the GFRP composite bridge model are quite less compared to those of obtained from the steel (Case 1) and Steel-GFRP (Case 3) bridge model. It can easily be seen that the shear forces and bending moments values at the pylon obtained Case 1 and Case 3 are nearly equal.
- The static analyses are performed to compare the analyses results. It is seen that the displacements and axial forces attained from the pylon are bigger for geometrically nonlinear analysis, the values of shear forces are nearly equal, and the bending moments are bigger for static analyses.
- The displacements increase along the bridge deck and reach a maximum of 5.7 cm at the middle for the Case 3. The displacements are very close to each other for all cases.
- The shear forces and bending moments are nearly equal for Case 2 and Case 3. The maximum shear forces and bending moments occurred as 339 kN and 660 kNm for Case 1, respectively. Numerical results indicated that the GFRP material (Case 2) has an important effect on the shear forces and bending moments.
- The static analyses are performed to compare the analyses results. It is seen that the displacements, shear forces and bending moments attained from the deck are smaller for geometrically nonlinear analysis.
- The hanger forces values obtained for Case 1 and Case 3 are nearly equal for all hangers. The maximum forces on the hangers occurred as an almost 70 kN for Case 1 and Case 3. On the other hand, the maximum hanger forces obtained for Case 2 occurred as 30 kN.
- The static analyses are performed to compare the analyses results. It is seen that the hanger forces are bigger for geometrically nonlinear analysis.

Geometrically nonlinear dynamic analyses

- The displacement and axial forces for the Case 1 are bigger than the corresponding response obtained for the Case 2 and Case 3. At the top of the bridge pylon, GFRP composite bridge model underestimates the responses by 36% and 70% relative to the steel bridge model case for displacement and axial force respectively.
- The axial forces are attained as -400 kN, -117 kN and -266 kN for Case 1, Case 2 and Case 3, respectively.
- The shear forces and bending moments obtained from the steel bridge model are bigger than the others. At the base of the bridge pylon, steel bridge model case overestimates the response by 76% relative to the GFRP bridge model case for shear force. In addition, steel bridge model overestimates the bending moment response by 75% relative to the GFRP bridge model at the top of the bridge pylon.
- The maximum displacements occurred as -4.9 cm, -3.5 cm and -2.6 cm at the middle of the bridge deck for the Case 1, Case 2 and Case 3 respectively. The results indicate that the GFRP material is more effective than the steel on the displacements of the deck as similar pylon dynamic displacements.
- The shear forces response values obtained from Case 1 are quite bigger than the corresponding response values obtained for the Case 2 and Case 3. The difference values of the maximum shear force between Case 1 and Case 2 are reached to approximately 88% at the abutment for the bridge deck.
- The bending moments obtained for the steel bridge model are quite bigger than the values obtained for the GFRP bridge model. The differences are reached to approximately 90% at the middle of the bridge deck.
- The GFRP material is more effective than the steel on the dynamic hanger forces as similar to internal forces.

Based on the results of this study, it can be said that there is a huge potential for the use of FRP composites for the footbridges applications thanks to beneficial properties and various advantages when these materials are compared to traditional ones.

References

- Adanur, S., Altunışık, A.C. and Keskin, A. (2010), "Comparison of analysis results of footbridges using steel and CFRP materials", *Proceedings of the 6th ASCE International Engineering and Construction Conference*, Cairo, Egypt, June.
- Adanur, S., Mosallam, A.S., Shinozuka, M. and Gumusel, L.A. (2011), "Comparative study on static and dynamic responses of FRP composite and steel Suspension bridges", *J. Reinf. Plastics Compos.*, **30**(15), 1265-1279.
- Aluri, S., Jinka, C. and GangaRao, H.V.S. (2005), "Dynamic response of tree fiber reinforced polymer composite bridges", *J. Mater. Civil Eng., ASCE*, **10**(6), 722-730.
- Alampalli, S. (2006), "Field performance of an FRP slab bridge", *Compos. Struct.*, **72**(4), 494-502.
- Aref, A.J. and Parsons, I.D. (2000), "Design and performance of a modular fiber reinforced plastic bridge", *Compos. Part B*, **31**(6-7), 619-628.
- Burgueno, R., Karbhari, V.M., Seible, F. and Kolozs, R.T. (2001), "Experimental dynamic characterization of an FRP composite bridge superstructure assembly", *Compos. Struct.*, **54**(4), 427-444.
- Caron, J.F., Julich, S. and Baverel, O. (2009), "Selfstressed bowstring footbridge in FRP", *Compos. Struct.*, **89**(3), 489-496.

- Chen, Y., Ziehl, P.H. and Harrison, K.W. (2009), "Experimental characterization and optimization of hybrid FRP/RC bridge superstructure system", *J. Bridge Eng., ASCE*, **14**(1), 45-54.
- Elsafi, O.H., Albers, W.F. and Alampalli, S. (2012), "Dynamic analysis of the Bentley Creek Bridge with FRP deck", *J. Bridge Eng., ASCE*, **17**(2), 318-333.
- Firth, I. and Cooper, D. (2002), "New materials for new bridges-Halgavor Bridge, UK", *Struct. Eng. Int.*, **12**(2), 80-83.
- Hodhod, O.A. and Khalifa, M.A. (1997), "Seismic performance of a fiber-reinforced plastic cable-stayed bridge", *Struct. Eng. Mech., Int. J.*, **5**(4), 399-414.
- Jin, F., Feng, P. and Ye, L. (2010), "Study on dynamic characteristics of light-weight FRP footbridge", *Proceedings of the 5th International Conference on FRP Composites in Civil Engineering*, Beijing, China, September.
- Khalifa, M.A., Hodhod, O.A. and Zaki, M.A. (1996), "Analysis and design methodology for an FRP cable-stayed pedestrian bridge", *Compos. Part B*, **27**(3-4), 307-317.
- Meiarash, S., Nishizaki, I. and Kishima, T.I. (2002), "Life-cycle cost of all-composite suspension bridge", *J. Compos. Constr.*, **6**(4), 206-214.
- Meier, U. (1987), "Proposal for a carbon fibre reinforced composite bridge across the Strait of Gibraltar at its narrowest", *Proceedings of the Institution of Mechanical Engineers, Part B: Journal of Engineering Manufacture*, Venue, May, **Volume 201**, 273-278.
- Potyrala, P.B. (2011), *Use of Fiber Reinforced Polymers in Bridge Construction: State of the Art in Hybrid and All-Composite Structures*, 93 p.
- Przemieniecki, J.S. (1968), *Theory of Matrix Structural Analysis*, Dover Publications, Mineola, NY, USA.
- SAP2000 (2008), *Integrated Finite Element Analysis and Design of Structures*, Computers and Structures Inc., Berkeley, CA, USA.
- Shrivastava, R., Gupta, U. and Choubey, U.B. (2009), "FRP: Research, education and application in India and China in civil engineering", *Int. J. Recent Trends in Eng.*, **1**(6), 89-93.
- Szak, P.J., Robson, B.N., Harik, I.E. and Brailsford, B. (1999), "The clear creek hybrid composite I-Girder pedestrian bridge", *J. Compos. Construct., ASCE*, **3**(2), 101-104.
- Votsis, R.A., Wahab, M.A. and Chryssanthopoulos, M.K. (2005), "Simulation of damage scenarios in a FRP composite suspension footbridge", *Key Eng. Mater.*, **293-294**, 599-606.
- Wang, X. and Wu, Z. (2010), "Integrated high-performance thousand-metre scale cable-stayed bridge with hybrid FRP cables", *Compos. Part B*, **41**(2), 166-175.
- Wang, X., Wu, Z., Wu, G., Zhu, H. and Zen, F. (2013), "Enhancement of basalt FRP by hybridization for long-span cable-stayed bridge", *Compos. Part B*, **44**, 184-192.
- URL (2012a), http://www.cosacnet.soton.ac.uk/presentations/5thMeet/cooper_5th.pdf
(Accessed on July 11, 2012)
- URL (2012b), PEER, Pacific Earthquake Engineering Research Centre (Accessed on December 24, 2012)
http://peer.berkeley.edu/nga_files/ath/KOCAELI/YPT330.AT2